ANALYTICAL SCIENCES APRIL 2017, VOL. 33

2017 © The Japan Society for Analytical Chemistry

Development of a High-Density Microplasma Emission Source for a Micro Total Analysis System

Ken KAKEGAWA,*† Ryoto HARIGANE, Mari AIDA,* Hidekazu MIYAHARA,* Shoji MARUO,** and Akitoshi OKINO***

**Laboratory for Future Interdisciplinary Research of Science and Technology, Tokyo Institute of Technology, 4259-J2-32 Nagatsuta, Midori, Yokohama, Kanagawa 226–8502, Japan*
***Department of Mechanical Engineering and Materials Science, Yokohama National University, 79-5 Tokiwadai, Hodogaya, Yokohama 240–8501, Japan*

To achieve a highly sensitive and onsite analysis of a small amount samples, a microplasma-based micro total analysis systems (μ-TAS) device was developed. A dielectric barrier discharge (DBD) that can generate a stable plasma at atmospheric pressure was generated in a microchip and used as the plasma source. The use of DBD suppresses the temperature rise of the electrodes and enables operation for long times because of a reduction of the electrode damage due to suppression of the current *via* dielectric interposing between the electrodes. It is expected that the analytical system can be miniaturized because helium plasma is generated in the microchannel contained in the microchip. Emissions from gaseous Cl, Br, and I were analyzed using the plasma source, and it was found that the detection limits for these analytes were 0.22, 0.18, and 0.14 ppm, respectively. The calibration curves for gaseous Cl, Br, and I were also plotted obtaining correlation coefficients of 0.975, 0.955 and 0.986, respectively, and showing good linearity for the developed plasma source.

Keywords Micro total analysis systems, μ-TAS, atmospheric plasma, micro plasma, gas analysis, atomic emission spectroscopy

(Received August 30, 2016; Accepted November 21, 2016; Published April 10, 2017)

Introduction

The development of highly sensitive, miniature systems for the analysis of small samples is required in medical and environmental fields. For example, such systems are expected to be applied to elemental analysis for the saliva as well as sweat and onsite[1–3] analysis for particulate matter in the atmosphere, such as PM 2.5.[4]

Recently, there has been increasing interest in the use of micro total analysis systems (μ-TAS) as miniaturized analytical systems for the analysis of small sample amounts.[5,6] The use of such a μ-TAS device enables the miniaturization of analytical systems, the reduction of the amount of samples necessary for analysis, and a decrease in the analysis time because each chemical analytical system element is integrated on a single chip using the micromachining technique. UV absorbance detection,[7] laser-induced fluorescence,[8,9] electrochemical detection[10,11] as well as other techniques have been used as the basis for μ-TAS detectors. Nevertheless, as shown by recent studies, these systems are currently limited by their inability to analyze a wide range of compounds and by their insufficient analytical sensitivity.

Inductively coupled plasma atomic emission spectrometry/mass spectrometry (ICP-AES/MS) has been widely used for the high-sensitivity analysis of trace elements.[12] In this method, a plasma with a volume of approximately 10 cm^3 excites and ionizes the samples. Recently, a microplasma, where the characteristic length of the plasma is on the order of micrometers, has attracted the attention of researchers in various fields; it has been used for hydrophilization of the surfaces of films,[13] and in medical applications for sterilization[14,15] and for atmospheric pressure desorption ionization.[16,17] The first report of microplasma used as an excitation source of μ-TAS was presented by Manz *et al.*[18] They generated a direct-current glow discharge in a glass chamber under decompression with a detection limit of 600 ppm, and detected methane. However, the lifetime of the system was approximately 2 h because the discharge electrodes were sputtered under decompression. Horiike *et al.* fabricated an atmospheric pressure ICP source in a discharge tube having dimensions of $1 \times 1 \times 30$ mm^3 (h/w/l).[19] The electron number density and excitation temperature were approximately 1×10^{15} cm^{-3} and 4500 K, respectively, using a compact VHF transmitter at a frequency and power of 144 MHz and 50 W, respectively. However, in this experiment, the temperature of the microchip increased to several hundred degrees with increasing temperature of the electrodes because of a large current flowing between the electrodes. Therefore, the power loss was large and the plasma could not be efficiently produced.

In this study, a microplasma source for a μ-TAS-incorporated microchip with a microchannel was developed. We used a dielectic barrier discharge (DBD) to generate a stable plasma at

† To whom correspondence should be addressed.
E-mail: k.kakegawa@plasma.es.titech.ac.jp

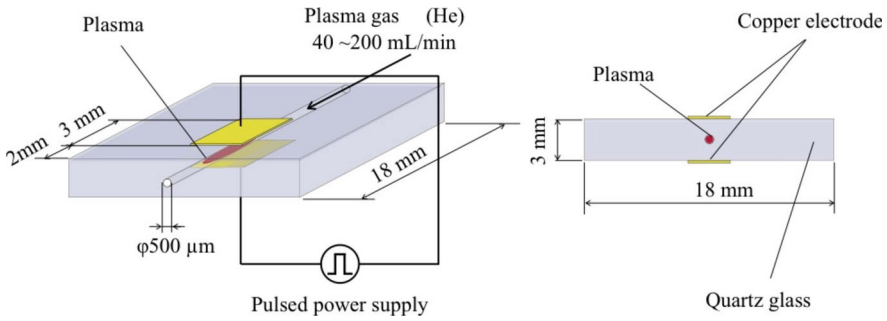

Fig. 1 Microplasma source for μ-TAS.

atmospheric pressure. Using the DBD approach, suppressing the temperature rise of the electrodes and operating it for a long time is possible because of suppression of the current and reduction of the electrode wear *via* dielectric interposition between the electrodes. In the developed plasma source, the plasma was also generated in the microchannel; the absence of a cell for plasma generation is advantageous for system miniaturization. The microchip was fabricated *via* a 3D molding process based on microstereolithography.[20,21] In this process, fabricating the microchip integrated with all elements necessary for analysis—such as the developed plasma source, sample introduction, and fluid control units—is possible because the microstructure can be constructed of various materials. To evaluate the basic performance of the fabricated system, the excitation temperature and the electron density of the plasma were spectroscopically measured. The detection limit and linearity of the calibration curves were also evaluated using the analysis of Cl, Br, and I content of air pollution fine particles as an example.

Experimental

Development of microplasma source for μ-TAS using 3D molding process based on microstereolithography

The configuration of our newly developed microplasma source is shown in Fig. 1. First, to fabricate the microchip, a polymer model of the microchannel shape was fabricated by microstereolithography. The parameters of the fabrication were adjusted so that the concentration of the ceramic powder would become highest. To fabricate the model, a He-Cd laser (IK5551R-F, KIMMON KOHA Co., Ltd., Japan) was used as the laser source. The resolution was 11 μm with the laser beam (wavelength, 325 nm; laser power, 0.8 – 0.9 mW) output passing from the He-Cd laser to the ND filter with a numerical aperture of 0.017. The polymer model was fabricated by irradiating the photopolymer (TSR-833, CMET Inc., Japan) with this laser. The cast material was composed of a muddy slurry comprising ceramic fine particles, pure water, and dispersant. SO-E2 (Admatechs, Co., Ltd., Japan) and D-735 (Chukyo Yushi, Co., Ltd., Japan) were used as ceramic fine particles and the dispersant, respectively. The weight ratios of ceramic fine particles, dispersant, and pure water were 10:0.2:2.55 (g). The fabricated polymeric mold was filled with the slurry by centrifuging. Next, the slurry was dried in a humidity-controlled oven at 35°C and humidity of 90% for 1 h, and was dried at of 80°C and a humidity of 35% for 24 h. Finally, the mold was decomposed by heating according to the temperature profile based on the master decomposition curve (MDC).[22] In the MDC method, by controlling the constant vaporization amount of the slurry per a unit of time, preventing damage caused by the rapid weight loss of the slurry is possible. As a result, the microchip with a microchannel with the diameter and length of 500 μm and 18 mm, respectively, was fabricated. In addition, a pair of 3-mm-long electrodes was placed on the microchip to generate the plasma in the microchannel. The helium gas flowed through the microchannel, and DBD plasma was generated by applying a square-wave voltage.

Spectroscopic characteristics

The basic performance of the developed microplasma for μ-TAS was investigated by spectroscopy. First, the transmittance of the fabricated microchip was measured using a spectrophotometer (UV-1700, Shimadzu, Inc., Japan) to verify whether the fabricated microchip can be used as the excitation source. Then, the excitation temperature and electron density of the plasma source were measured. A high-voltage power supply (PCT-MBS-50kai, Plasma Concept Tokyo, Inc., Japan) was used to generate the plasma with an applied voltage and frequency of 7 kV and 15 kHz, respectively. In this study, to prevent damage of the microchannel, a low discharge power and frequency were used. Emission intensity will increase with the discharge power and the frequency. The gas flow rate was varied from 40 to 200 mL/min because the plasma performance was dependent on the gas flow rate. To observe the emission from the plasma, an optical fiber was aligned with the axis of the plasma, and the spectra were recorded using a multichannel spectrometer (HR400, 424.07 – 506.79 nm, Ocean Optics, Inc., USA). The tip of the optical fiber was located 2.5 mm from the plasma exit. The excitation temperature was determined from a Boltzmann plot of the emission intensity ratio of the He I line at 477.148, 492.193, and 501.568 nm. The electron density was determined by evaluating the Stark broadening of the H_β line at 486.133 nm.

Microplasma atomic emission spectroscopy

The gas sample was analyzed using the developed atomic emission source as the excitation source for μ-TAS. A schematic of the experimental setup is shown in Fig. 2. The spectra and detection limit of gaseous Cl were investigated using the applied voltage, frequency, and gas flow rate of 7 kV, 15 kHz, and 40 – 200 mL/min, respectively. To prepare the analyte sample, 11 μL of CH_2Cl_2 (Wako Pure Chemical Industries, Ltd., Japan) was injected and vaporized in a 100-mL vessel filled with He. Next, the gaseous sample was filled into a microsyringe and was mixed with plasma gas using a syringe pump (Model 100 Series, kD Science Inc., USA). The flow rate of the syringe pump was controlled until a concentration of 40 ppm of the gas sample was introduced into the plasma. The emission spectra were

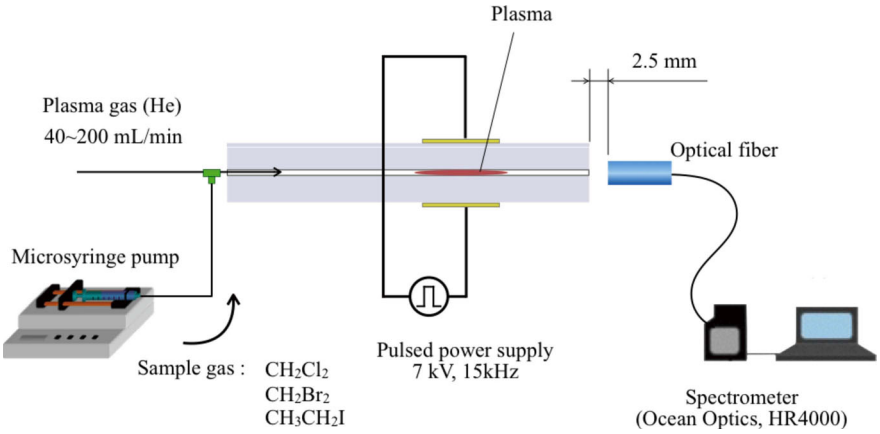

Fig. 2 Schematic of the analytical system for gas samples using the microplasma.

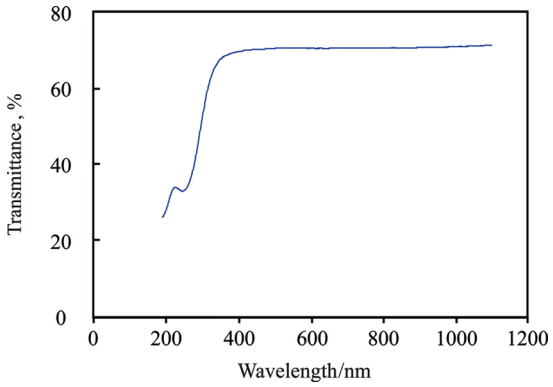

Fig. 3 Measured transmittance of the fabricated microchip.

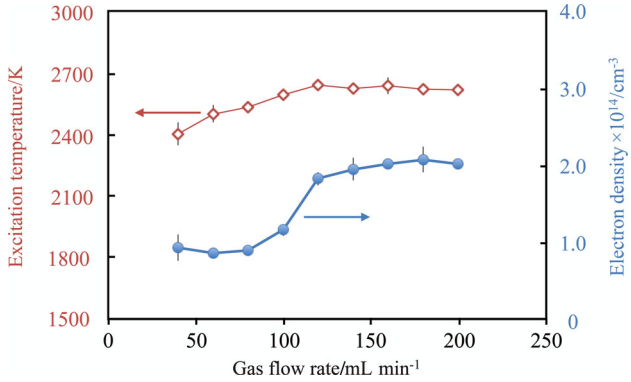

Fig. 4 Excitation temperature and electron density of the developed plasma source.

measured using a multichannel spectrometer (HR400, 548.16 – 1002.58 nm, Ocean Optics, Inc., USA) and the position of the optical fiber was as specified above. Gaseous Br and I were also analyzed, and their detection limits were determined with a gas flow rate of 140 mL/min. To prepare the gaseous Br and I, CH_2Br and C_2H_5I (Wako Pure Chemical Industries, Ltd., Japan) were used. Next, calibration curves for Cl, Br, and I were determined for the applied voltage, frequency, and gas flow rate of 7 kV, 15 kHz, and 140 mL/min, respectively.

Results and Discussion

Fundamental investigations of the microplasma

Figure 3 shows the transmittance of the fabricated microchannel. The transmittance was approximately 70% from 340 to 1100 nm. Although the microchannel transmittance was slightly lower that of the quartz glass, plasma emission transmitted through the microchip in the wavelength range of interest. This enabled radial photometry for the performance of emission spectrometry in the radial direction of the plasma as well as axial photometry for the performance of emission spectrometry in the axial direction of plasma. For axial photometry, highly sensitive analysis is possible because of the long photometric region relative to the radial photometry. On the contrary, positions showing strong emissions are different between the samples due to the varying temperature and density of the plasma in the axial direction. Therefore, an accurate analysis of the sample can be expected for radial photometry even if spectral interference is present in axial photometry. In this experiment, emission spectrometry was performed using axial photometry to achieve the high sensitivity necessary for the analysis of trace elements.

The excitation temperature and the electron density of the plasma measure the excitation performance and the reaction frequency of the samples, and are therefore highly important parameters for plasma evaluation. Figure 4 shows the variation of the excitation temperature and the electron density for the applied voltage, frequency, and gas flow rate of 7 kV, 15 kHz, and 40 – 200 mL/min, respectively. The excitation temperature and electron density increased until obtaining a plasma gas flow rate of 140 mL/min. However, as the gas flow rate increased further, these parameters remained almost constant at 2600 K and 2.0×10^{14} cm^{-3}, respectively. This is because the ionized or excited He atoms were nearly saturated in the microchannel at a rate of 140 mL/min despite the increase in their amount with further increases of the gas flow rate. The excitation temperature and the electron density of He-ICP were 3600 K and 0.42×10^{14} cm^{-3}, respectively.[23] A comparison of the He-ICP to the developed plasma source shows that the excitation temperature of the developed plasma source was lower by 1000 K, but the electron density was increased by approximately a factor of 5. In the He-ICP, the plasma volume and the power were 3 cm^3 and

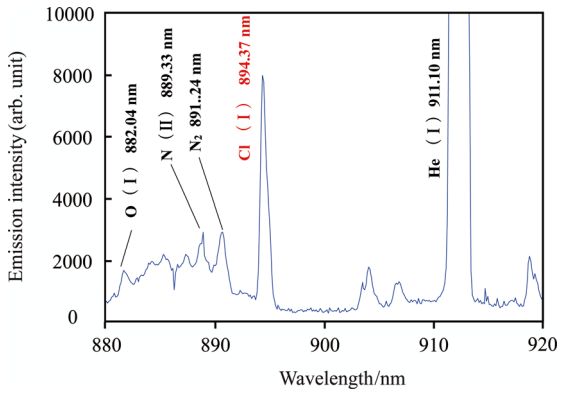

Fig. 5 Emission spectra of CH_2Cl_2 (40 ppm).

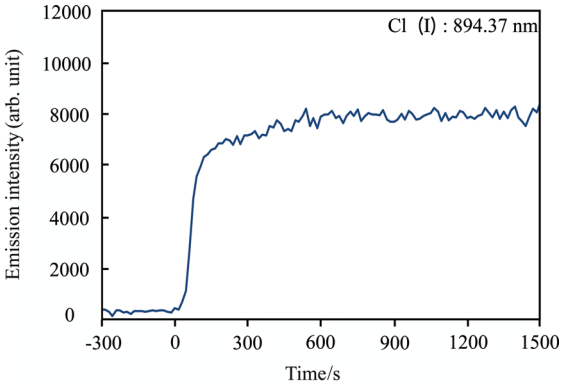

Fig. 6 Elapsed time of of 894.37-nm Cl (40 ppm).

700 W, respectively.[23] In this plasma source, they were 6×10^{-4} cm^3 and 0.8 W, respectively. Thus, their power densities were 230 W/cm^3 and 1300 W/cm^3. This will be the cause of higher electron number density.

Previous studies showed that in a microplasma, the ionization/excitation of He atoms cannot be sufficiently performed because the residence time in the plasma is extremely short in the case of a high plasma gas flow rate.[24] Therefore, the plasma gas flow rate was 40 – 200 mL/min in the following experiments. Assuming that the plasma gas temperature was 45°C,[16] the sample residence time in the plasma was 0.83 – 0.17 ms.

Atomic emission spectroscopy using the microplasma

Emission spectrometry of 40-ppm gaseous Cl was performed at a plasma gas flow rate of 140 mL/min with the results presented in Fig. 5, demonstrating successful detection of the Cl atomic line at 894.37 nm. Figure 6 shows the elapsed time of the Cl emission intensity; 0 min of the horizontal axis shows the start time of introducing Cl. The emission intensity of Cl rose in 20.3 s from the sample introduction. This is almost the same as the sample flow time in the gas tube. The rise time of the emission was 59.1 s and the emission intensity of Cl was almost constant after 600 s. It is believed that in addition to affecting the density and temperature of the plasma, the plasma gas flow rate influences the residence time of the samples in the plasma and detection of the samples. Therefore, the relations between the plasma gas flow rate and the emission intensity and detection limit of Cl were examined; the results are shown in Fig. 7. The detection limit was determined for $S/N = 3$, where S is the

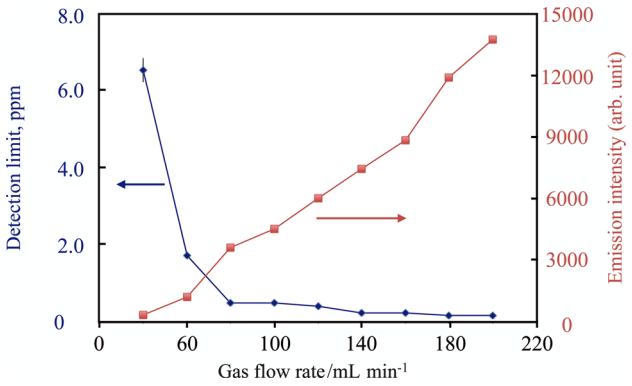

Fig. 7 Detection limit and emission intensity of 894.37-nm Cl obtained for different gas flow rates.

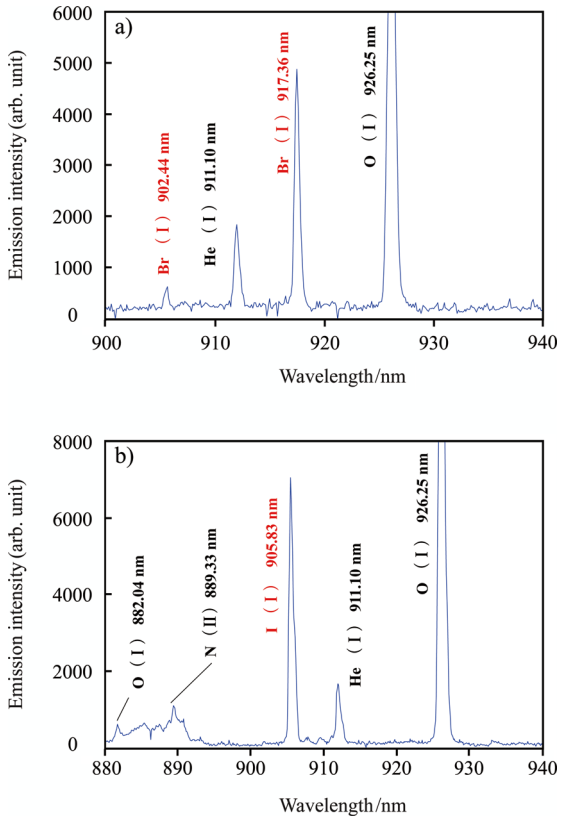

Fig. 8 Emission spectra of (a) CH_2Br_2 and (b) C_2H_5I.

detected signal intensity and N (noise) is the standard deviation of the background signal intensity. As the plasma gas flow rate increased, the Cl emission intensity increased and the Cl detection limit decreased. The detection limit rapidly decreased in the flow rate range of 40 – 80 mL/min, and then gradually decreased in the 80 – 140 mL/min range. On the contrary, the Cl emission intensity increased after 140 mL/min. A comparison of Figs. 4 and 7 shows that the excitation of the sample influences the other high-energy particles in the plasma as well as excited He atoms because the excitation temperature and electron density remains almost constant after 140 mL/min.

Next, the emission spectra of 40-ppm gaseous Br and I at the plasma gas flow rate of 140 mL/min were obtained; as shown in

Table 1 Detection limit of gaseous Cl, Br and I

Sample	Measurement wavelength/nm	Detection limit, ppm
CH_2Cl_2	Cl(I) 837.37	0.22
CH_2Br_2	Br(I) 917.36	0.14
CH_2CH_2I	I(I) 905.83	0.18

Fig. 8, the Br and I atomic lines were successfully detected at 917.36 and 905.83 nm, respectively. The detection limits of the Br 917.36-nm and I 905.83-nm lines were 0.18 and 0.14 ppm, respectively. Based on the data presented in Fig. 7, a detection limit of 0.22 ppm was obtained for Cl. These results are given in Table 1. Therefore, iodine can be detected with the smallest sample volume, while the detection of chlorine requires the highest sample amount. This is due to the differences in the ionization energies of chlorine, bromine, and iodine, which are 13.0, 11.8, and 10.5 eV, respectively, giving rise to the detection limit decreasing with the lower ionization energy in the order of chlorine, bromine, and iodine. A comparison to the detection limit of the gas chromatography thermal conductivity detector (GC-TCD) used as a general gas detector shows the advantages of the developed system. The detection limit for GC-TCD is approximately 1 ppm, a factor of 5 – 7 higher than the detection limits observed for Cl, Br, and I using the developed system. This demonstrates the usefulness of the developed microplasma-based system for analysis of small sample amounts.

Linearity of calibration curves

Calibration curves were plotted for each gas sample using the atomic beams of Cl 894.37 nm, Br 917.36 nm, and I 905.83 nm lines. The concentration of each gas sample varied from 0 to 150 ppm; the obtained calibration curves are shown in Fig. 9. The correlation coefficients for Cl, Br, and I were 0.975, 0.986 and 0.995, respectively, showing that good linearity was obtained. In the low concentration region, the calibration curve was almost linear to the detection limit, and the linearity was not inhibited. However, the linearity was inhibited in the high concentration region. This is considered to be the limit of the excitation performance, depending on the intensity of a discharge rather than the influence of self-absorption. Because in this study, the resonant line was not used; for example, in case of Cl analysis, 894.81 nm of the non-resonant transition from $3s^23p^44s$ to $3s^23p^44p$ was measured. A linearity of 2 digits was obtained for chlorine and iodine, and a linearity of 3 digits was obtained for bromine. In conventional argon ICP, the decomposition and ionization rates of halogens are not very high. The ionization rates of chlorine, bromine and iodine are reported to be 1.4, 7.2 and 36.1%, respectively.[25] The sample residence time in ICP is about 1.5 ms. In the developed plasma source, all of halogen samples may not have been decomposed and excited because the sample residence time was about 0.24 ms. However, quantitative analysis of the samples is possible because of the linearity of calibration curves. The general GC-TDC has a linearity of 5 – 6 digits; hence, in a future study, considering an improvement of dynamic range performing radial photometry is necessary.

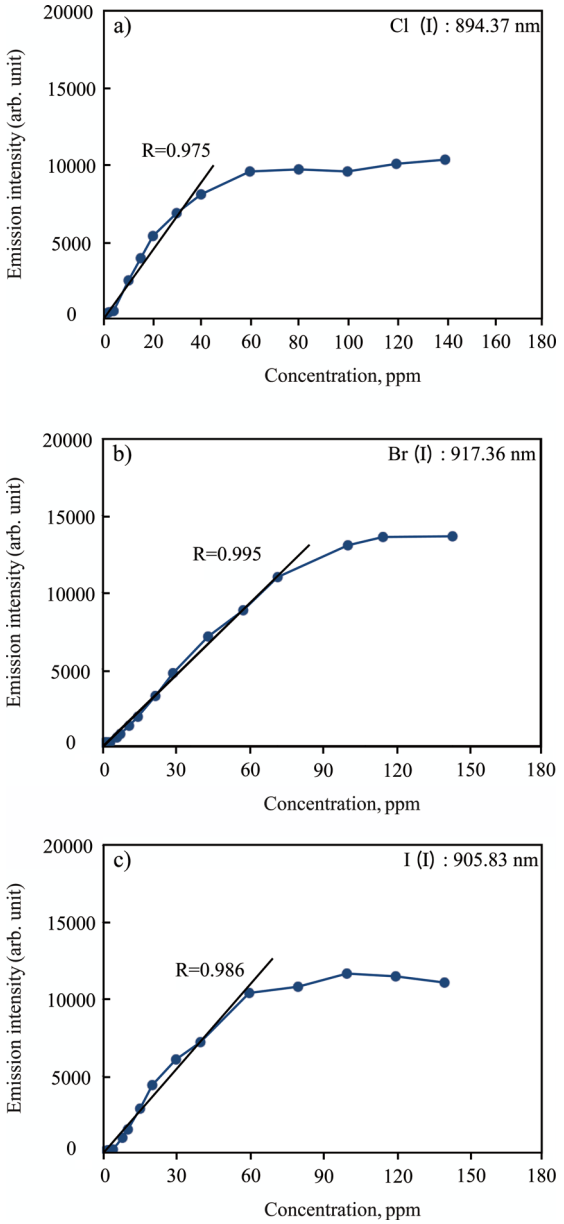

Fig. 9 Calibration curves for (a) chlorine, (b) bromine, and (c) iodine.

Conclusion

In this study, to perform high sensitivity analysis for small sample amounts, a microplasma source for μ-TAS was developed. First, a microchip with a microchannel of 500 μm at the center was fabricated using a 3D molding process based on microstereolithography. To generate a plasma, copper electrodes were placed on the microchannel, and a square wave having a voltage and frequency of 7 kV and 15 kHz, respectively, was applied. The excitation temperature and the electron density of the plasma obtained using He gas were 2300 K and 2.0×10^{14} cm^{-3}, respectively. To understand the plasma properties, distribution measurements of the plasma temperatures and the electron number density are required. To measure that, we must use micro and time resolved spectroscopy. In our future study, that will be investigated. The gaseous chlorine, bromine, and iodine were analyzed using the plasma source as the excitation source; detection limits of 0.22, 0.14, and 0.18 ppm, respectively, were obtained for these analytes. The obtained detection limits are smaller than the approximately 1-ppm detection limit of GC-TCD, demonstrating the usefulness of the developed system. The calibration curves for these

analytes were also plotted, and a linearity of 2 digits was obtained for chlorine and iodine and that of 3 digits was obtained for bromine. In this study, the diameter and the length of the plasma source were not optimized. They will be optimization in our future work.

References

1. S. Sugase and T. Tsuda, *Bunseki Kagaku*, **2002**, *51*, 429.
2. M. H. H. Ensom, T. K. H. Chang, and P. Patel, *Clin. Pharmacokinet.*, **2001**, *40*, 783.
3. R. Gorodischer, P. Burtin, Z. Verjee, P. Hwang, and G. Koren, *Ther. Drug Monit.*, **1997**, *19*, 637.
4. E. Yamada, K. Matsushita, M. Nakamura, Y. Fuse, S. Miki, H. Morita, and O. Shimada, *Chem. Lett.*, **2005**, *34*, 772.
5. P. N. Nge, C. I. Rogers, and A. T. Woolley, *Chem. Rev.*, **2013**, *113*, 2550.
6. D. R. Reyes, D. Iossifidis, P. A. Auroux, and A. Manz, *Anal. Chem.*, **2002**, *74*, 2623.
7. C. Ericson, J. Holm, T. Ericson, and S. Hjerten, *Anal. Chem.*, **2000**, *72*, 81.
8. J. Qin, Y. Fung, D. Zhu, and B. Lin, *J. Chromatogr. A*, **2004**, *102*, 223.
9. J. C. Sanders, Z. Huang, and J. P. Landers, *Lab Chip*, **2001**, *1*, 167.
10. J. Wang, B. Tian, and E. Sahlin, *Anal. Chem.*, **1999**, *71*, 3901.
11. J. Wang, M. Pumera, M. P. Chatrahi, A. Rodrigez, S. Spillman, R. S. Marin, and S. M. Lunte, *Electroanalysis*, **2002**, *14*, 1251.
12. K. Shigeta, H. Traub, U. Panne, A. Okino, L. Rottmann, and N. Jakubowskia, *J. Anal. At. Spectrom.*, **2013**, *28*, 646.
13. T. Takamatsu, H. Hirai, R. Sasaki, H. Miyahara, and A. Okino, *IEEE Trans. Plasma Sci.*, **2013**, *41*, 119.
14. T. Takamatsu, H. Miyahara, T. Azuma, and A. Okino, *J. Toxicol. Sci.,* **2013**, *39*, 281.
15. T. Oshita, H. Kawano, T. Takamatsu, H. Miyahara, and A. Okino, *IEEE Trans. Plasma Sci.*, **2015**, *43*, 1987.
16. T. Iwai, Y. Takahashi, H. Miyahara, and A. Okino, *Anal. Sci.*, **1999**, *29*, 1141.
17. T. Iwai, K. Kakegawa, M. Aida, H. Nagashima, T. Nagoya, M. Kanamori-Kataoka, H. Miyahara, Y. Seto, and A. Okino, *Anal. Chem.*, **2015**, *87*, 5707.
18. J. C. T. Eijkel, H. Stoeri, and A. Manz, *Anal. Chem.*, **1999**, *71*, 2600.
19. T. Ichiki, T. Koidesawa, and Y. Horiike, *Plasma Sources Sci. Technol.*, **2003**, *12*, S16.
20. S. Maruo, *SPIE Newsroom*, **2012**, 29.
21. M. Inada, D. Hiratsuka, J. Tatami, and S. Maruo, *Jpn. J. Appl. Phys.*, **2009**, *48*, 06FK01.
22. C. B. DiAntonio, K. G. Ewsuk, and D. Bencoe, *J. Am. Ceram. Soc.*, **2005**, *88*, 2722.
23. A. Okino, H. Ishizuka, I. Hirayama, Y. Nomura, and R. Shimada, *Bunseki Kagaku,* **1994**, *43*, 685.
24. H. Eguchi, K. Nakamura, F. Endo, T. Nishiyama, T. Nakagawa, N. Seino, M. Sinoda, and K. Uchiyama, *Bunseki Kagaku*, **2005**, *54*, 869.
25. H. Haraguchi, "*Basic and Application for ICP Atomic Emission Spectrometry*", **1986**, Kodansha Ltd.